HEFAT2012
9th International Conference on Heat Transfer, Fluid Mechanics and Thermodynamics
16 – 18 July 2012
Malta

HEAT TRANSFER IN TURBULENT FLOWS WITH LAGRANGIAN METHODS: SCALES OF TURBULENT TRANPORT IN WALL TURBULENCE

Papavassiliou D.V. * and Srinivasan C.
*Author for correspondence
Department of Chemical, Biological and Materials Engineering,
University of Oklahoma,
Norman, Oklahoma, 73072,
United States of America,
E-mail: dvpapava@ou.edu

ABSTRACT

We use a Lagrangian computational methodology that allows the calculation of statistical quantities in turbulent heat transfer. The study utilizes a direct numerical simulation (DNS) of turbulent flow in an infinite channel and in plane Couette flow, in conjunction with the Lagrangian scalar tracking method (LST). The computational box dimensions are $4\pi h \times 2h \times 2\pi h$ in x, y, z for Poiseuille flow and $8\pi h \times 2h \times 2\pi h$ for Couette flow (where h is the half channel height). The transport of heat is simulated with LST, which involves the tracking of the trajectories of heat markers in the flow generated by the DNS. The effects of convection are simulated by moving the markers under the assumption that they follow the velocity field. The diffusion effect is simulated by adding a 3D random walk on the particle motion that follows a normal distribution with a standard deviation that depends on the Prandtl number, Pr, of the fluid [1]. The range of Pr covers a wide range (between 0.1 and 6). The trajectories of about 150,000 heat markers are calculated for each case. These trajectories are then used to obtain turbulent dispersion data and to obtain the correlation coefficients for single particle and for relative particle pair dispersion. In addition, the dispersion backwards in time was considered. This was motivated by recent studies about backwards dispersion that have shown differences with forwards turbulent dispersion. The results show differences in the rates of forwards and backwards dispersion [2]. The time scales that are important to turbulent transport and for mixing are thus revealed. Differences between Couette flow and Poiseuille flow highlight the effects of the velocity structure of the turbulence next to the wall on the transport of heat. The presentation will present the numerical methodology and results will be compared with available data from earlier DNS works [3,4].

INTRODUCTION

Turbulent dispersion is one of the defining characteristics of turbulence and it plays a major role in many industrial applications involving heat exchange, mixing, flow in reactors or catalyst regeneration units. Accurate modelling of turbulent scalar transport is also critical for predicting environmental transport, such as bioagent or pollutant dispersion in the atmosphere. Depending on whether one analyzes a single particle or pairs of particles selected from a particle cloud undergoing dispersion, single or relative dispersion, respectively, are of interest. In addition to this, two different forms of turbulent dispersion can be distinguished, depending on the timeframe of dispersion that is of interest. Forwards dispersion can be identified as the dispersion of interest when the scalar markers diffuse away from the same source point (or volume). A typical example is the smoke emanating from a chimney. The backwards dispersion, on the other hand, is the dispersion of interest when the scalar markers are diffusing towards a particular location in the flow field. Combining these two dispersion cases with the possibility of studying one or pairs of scalar markers, one can study the forwards and backwards single particle or relative dispersion, respectively.

Few previous studies have been devoted to the understanding of backwards dispersion, and analyzing it's behaviour with respect to forwards dispersion. Bernard and Rovelstad [5] were the first to perform direct numerical simulation to study single-particle backwards dispersion in a turbulent channel flow. They looked at an ensemble of fluid particles having common end points and studied the scalar transport correlations. Sawford et al. [6] studied two-particle relative dispersion in the inertial range using two different Lagrangian stochastic models and concluded that the backwards relative dispersion proceeds twice as fast as forwards dispersion for asymmetric turbulence. Experimental evidence of the differences between forwards and backwards

relative dispersion has been reported in the work of Berg et al. [7]. The results obtained showed that the backwards relative dispersion proceeds twice as fast as the forwards relative dispersion.

Early works in our laboratory studied the differences in the rates of backwards and forwards single marker dispersion in anisotropic wall-turbulence. The results showed that the extent of forwards or backwards dispersion was dependent on the distance from the channel walls and on the direction of dispersion. Also the *Pr* was found to affect the rates of the dispersion. Further studies found differences in the direction of scalar transport in case of forwards and backwards single marker dispersion and associated it with the coherent structures existing in such anisotropic flows. The recent focus of the work has shifted to also understanding if the turbulent forwards and backwards relative scalar dispersion shows any effects observed in the single marker scalar dispersion statistics. This conference paper will discuss the two-fold detail of the simulation methodology and some important results obtained for this study.

NOMENCLATURE

h	half channel height
Pr	Prandtl number
q	Heat flux
t	Time
u, v, w	fluctuating velocity components in x, y, z directions
x, y, z	streamwise, normal and spanwise coordinates
Special characters	
Δt	Time step
ν	Viscosity
π	Trigonometric pi (3.14159….)
Subscripts	
$()^+$	Values made dimensionless with wall parameters
$()_b$	Value for backwards dispersion
$()_f$	Value for forwards dispersion

NUMERICAL METHOD

Combined Direct Numerical Simulation (DNS)/Lagrangian Scalar Tracking (LST) method

The pseudospectral algorithm of Lyons et al. [8] is used to determine the velocity field for the Poiseuille channel flow, with an adjustment for plane Couette flow, where the walls of the channel move relative to each other. The fluid in both cases is considered to be an incompressible Newtonian fluid with constant density, constant viscosity and constant thermal conductivity. The viscous heating effects and the body forces are neglected. The no-slip, no-penetration boundary conditions are imposed at the walls of the channels, while periodic boundary conditions are imposed in the streamwise and spanwise directions. In Poiseuille channel flow, the simulation is carried out in a computational box with dimensions ($4\pi h^+$, $2h^+$, $2\pi h^+$), in the x, y and z directions, where two cases of h^+ = 150 and 300 viscous wall units were considered. The box is meshed with 128 × 65 × 128 and 256 × 129 × 256 mesh points, in the x, y, z directions, respectively, for h^+ = 150 and 300, respectively. For plane Couette flow, the length of the box is doubled in the x direction, with the computational box in the case of plane Couette flow measuring $8\pi h^+$, $2h^+$, $2\pi h^+$ in x, y and z directions, respectively, with h^+ = 150 and 256 × 65 × 128 grid points.

By tracking the trajectories of the scalar makers released into this flow field, the Lagrangian scalar tracking (LST) [9] method is used to determine the scalar dispersion statistics. The method of stochastically tracking the scalar markers combined with statistical post-processing of the results is termed Lagrangian scalar tracking (LST). According to this method, the scalar marker moves by the combination of convection, determined from the velocity of the fluid element on which the marker rides, and from molecular diffusion, obtained from a Gaussian distribution of zero mean and standard deviation $\sqrt{(2\Delta t)/\mathrm{Pr}}$ for each of the three coordinate directions. This molecular diffusion step, which is a function of *Pr*, helps to carry out simulations with different *Pr* (*Pr* = 0.1, 0.7, and 6). In the remainder of the manuscript, any reference to heat transfer in terms of *Pr* also applies to corresponding mass transfer in terms of Schmidt number (*Sc*). The number of scalar markers is 260100 and 145161, for the h^+ = 300 and 150, respectively. A detailed description of the application of DNS/LST to determine scalar dispersion statistics has been presented in previous works from our laboratory [1,10,11,12].

Simulating Forwards/Backwards Dispersion

Different regions of the channel present different scenarios and different physics in cases of forwards and backwards turbulent dispersion. In order to concentrate on a region, the channel in the vertical direction for small h^+ = 150, for both Poiseuille and plane Couette flow is divided into 101 uniform bins, while in the case of h^+ = 300, it is divided into 201 bins. Bins corresponding to four regions of turbulent channel flow, the viscous sub-layer, the transition region, the logarithmic region and the center of the channel, are studied particularly with interest. For conciseness, just the result for the viscous sub-layer and the center of the channel are presented here in this paper. In order to calculate forwards and backwards dispersion statistics, position and velocity of all the markers in the flow field at each time are stored in a database. At a particular time, the time of interest, referred to as *zero-time* from here on, and a particular bin of interest, the total number of markers present in the bin and the associated marker identity of each marker are determined. The trajectory of each of these markers prior to arriving in the bin can be obtained from previously stored data. The backwards single marker dispersion statistics is obtained by looking at the position and the velocity of a particular marker with respect to its position and velocity at at zero-time. In Figure 1 a pictorial representation of the *xy* view is offered, with the vertical direction sliced into bins, for the process of backwards single marker dispersion for markers moving towards the logarithmic region in the case of *Pr* = 0.1.

In the case of backwards relative dispersion, the particular marker position and velocity are analyzed with respect to the position and velocity of another marker. Figure 2 is a presentation of the case of relative dispersion for marker pairs moving towards three different regions of the channel. For complete details of this methodology refer to the previous work in our laboratory [8,9].

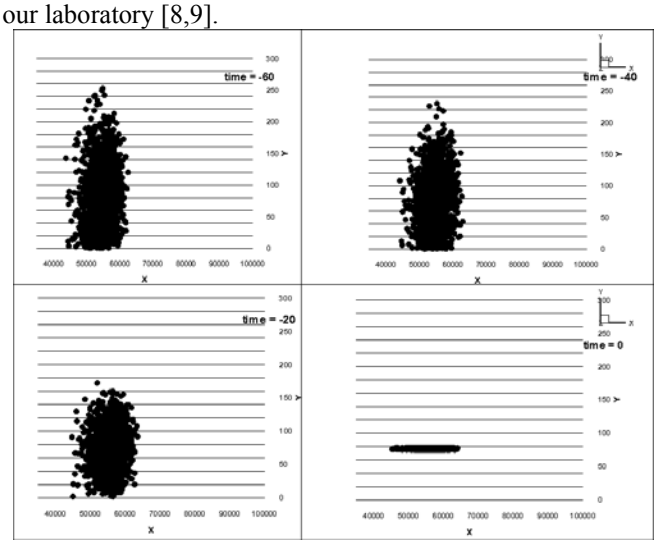

Figure 1. Scalar markers moving towards a particular bin (in this case located in the logarithmic region), for Poisueille channel flow, for $h^+ = 150$, as time evolves, in case of $Pr = 0.1$.

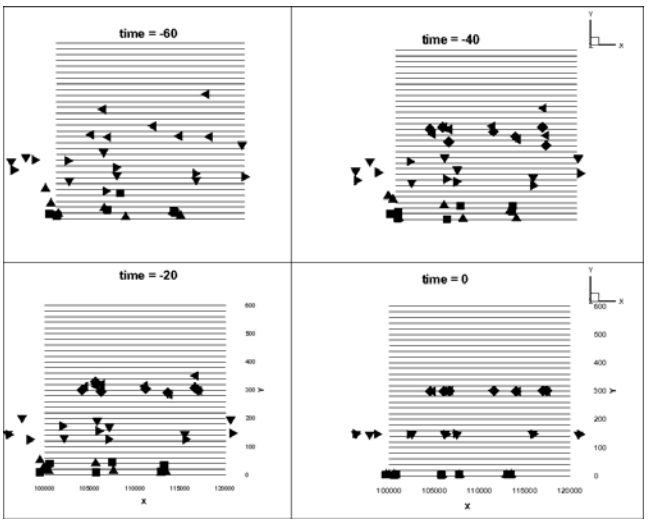

Figure 2. Pairs of scalar markers moving towards particular bins (in this case the bins are located in the viscous sub-region, logarithmic region and center of the channel), for Poiseuille channel flow, for $h^+ = 300$, as time evolves, in the case of $Pr = 0.1$.

RESULTS

In order to quantify the differences between the forwards and backwards dispersion, the differences in the value of mean squared displacement in the vertical, anisotropic direction, for the two cases is plotted as a function of time for different *Pr*. The mean squared displacement can be used to directly visualize the dispersion rate, hence, the differences in the mean square displacement reflect the differences in the rates of forwards and backwards dispersion. Figure 3 shows the differences between forwards and backwards single marker dispersion with the change of time for three $Pr = 0.1$, 0.7 and 6, with the markers captured in the *viscous* sub-range shown in (a) and the center of the channel in (b). The results indicate that the markers moving away from the viscous sub-regions are dispersing faster than those arriving at those locations while in the case of the center of the channel, this trend is reversed. The results also show that with increase in *Pr*, there is a percentage increase in the differences with $Pr = 0.1$, showing the least differences for both regions.

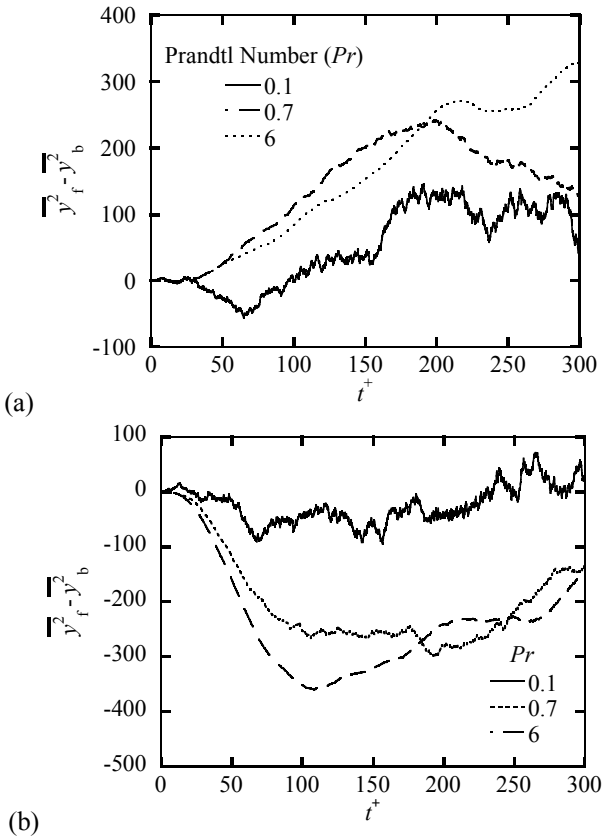

Figure 3. Differences between forwards and backwards single marker dispersion as a function of time for different *Pr*; in Poiseuille channel flow, with $h^+ = 150$; (a) viscous sub-layer; (b) center of the channel (data taken from ref. [11]).

In order to study the effects of *Re* in the rates of forwards and backwards dispersion and to observe how the relative dispersion behaves compared to single marker dispersion, Figure 4 shows the values of mean squared relative displacement as a function of time, for the same three *Pr* cases, with the viscous sub-layer plotted in (a) and the center of the channel in (b). It is very clear that the *Re*, considering a particular *Pr*, helps in increasing the differences in the rates of the forwards and backwards dispersion. Also, the single marker dispersion characteristics are very similar to the relative dispersion characteristics.

In order to understand the effect that a different flow structure has on the rates of forwards and backwards dispersion, the plane Couette flow is also studied. Very interestingly, in Figure 5, we see that the trend of rates of forwards and backwards relative dispersion, are reversed in this type of flow, compared to the Poiseuille flow. The viscous sub-regions show faster backwards relative dispersion while the center of the channel shows faster forwards relative dispersion.

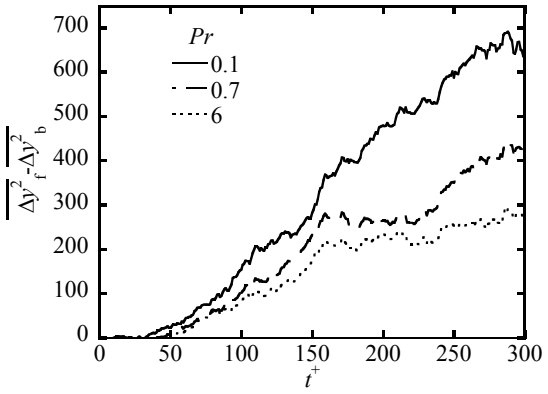

(a)

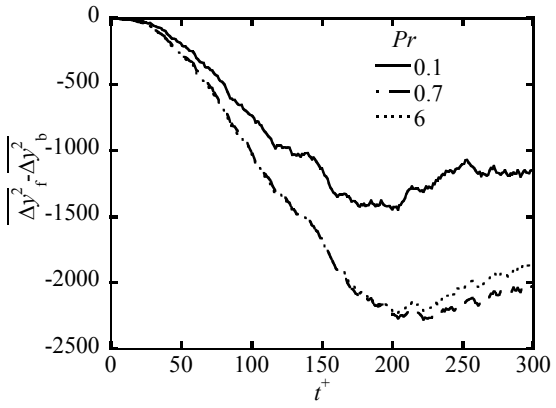

(b)

Figure 4. Differences between forwards and backwards relative dispersion as a function of time for different *Pr*, in Poiseuille channel flow, with $h^+ = 300$; (a) viscous sub-layer; (b) center of the channel.

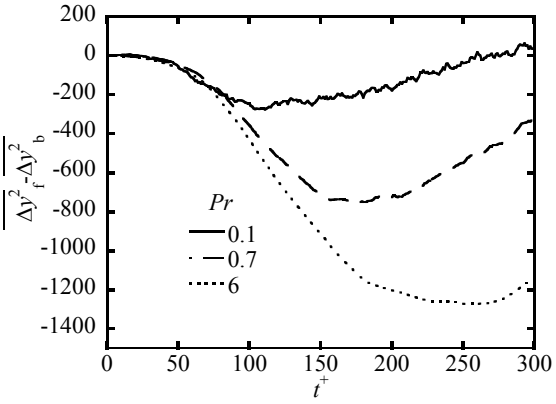

(a)

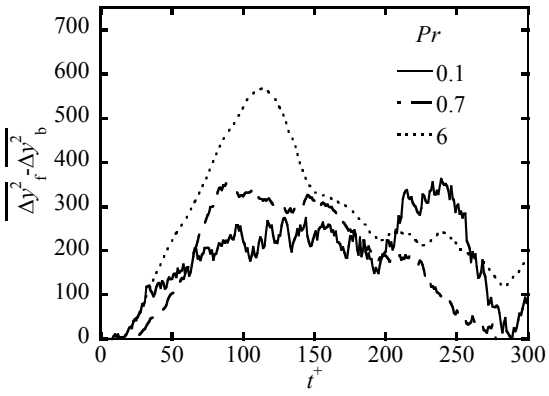

(b)

Figure 5. Differences between forwards and backwards relative dispersion as a function of time for different *Pr,* in plane Coeutte flow, with $h^+ = 150$; (a) viscous sub-layer; (b) center of the channel.

CONCLUSION

A combined DNS/LST approach is used in this study to understand scalar dispersion statistics for single marker and relative scalar dispersion. This method provides a very suitable framework to understand the scalar backwards dispersion, an alternate perspective of turbulent dispersion which is relevant to cases of turbulent mixing. This study outlines the simulation methodology utilized to analyze turbulent backwards dispersion in our laboratory. Some of the interesting results for dispersion rates obtained for turbulent single marker and relative dispersion, in cases of Poiseuille flow and plane Couette flow, for some cases of *Pr* are presented. The results show an increase in differences of forwards and backwards dispersion, for both single marker and relative dispersion, with an increase in the *Re*. The plane Couette flow and Poiseuille channel flow are also revealed to have some important difference in dispersion. The change in *Pr* show systematic changes in differences between the rates of forwards and backwards dispersion.

REFERENCES

[1] Mitrovic B.M., Le P.M., Papavassiliou D.V., On the Prandtl or Schmidt number dependence of the turbulent heat or mass transfer coefficient, Chemical Engineering Science, Vol. 59, No. 3, 2004, pp. 543-555.

[2] Srinivasan, C., and Papavassiliou, D.V., Direction of scalar transport in turbulent channel flow, Physics of Fluids, Vol. 23, No. 115105, 2011, pp. 1-20.

[3] Hasegawa, Y., and Kasagi, N., Low-pass filtering effects of viscous sub-layer on high Schmidt number mass transfer close to a solid wall, International Journal of Heat and Fluids Flow, Vol. 30, No.3, 2009, pp. 525-533.

[4] Sawford B.L., Yeung P.K., and Hackl, J.F., Reynolds number dependence of relative dispersion statistics in isotropic turbulence, Physics of Fluids, Vol. 20, No. 065111, 2008, pp. 1-13.

[5] Bernard P.S., and Rovelstad A.L., On the physical accuracy of scalar transport modeling in inhomogeneous turbulence, Physics of Fluids, Vol. 6, 1994, pp. 3093-3108.

[6] Sawford B.L., Yeung P.K., and Borgas M.S., Comparison of backwards and forwards relative dispersion in turbulence, Physics of Fluids, Vol. 17, 2005, pp. 095109 (1-9).
[7] Berg J., Lüthi B., Mann J., and Ott S., Backwards and forwards relative dispersion in turbulent flow: An experimental investigation, Physical Review E, Vol. 74, 2006, pp. 016304(1-7).
[8] S.L. Lyons S.L., T.J. Hanratty T.J., J.B. McLaughlin J.B., Large-scale computer simulation of fully-developed turbulent channel flow with heat transfer, International Journal of Numerical Methods in Fluids, Vol. 13, 1991, pp. 999-1028.
[9] K. Kontomaris, T.J. Hanratty, J.B. McLaughlin, An algorithm for tracking fluid particles in a spectral simulation of turbulent channel flow, Journal of Computational Physics 103 (1993) 231-242.
[10] Le P.M., and Papavassiliou D.V., Turbulent dispersion from elevated sources in Channel and Couette flow, AIChE Journal, Vol. 51, No. 9, 2005, pp. 2402-2414.
[11] Srinivasan C., and Papavassiliou D.V., Backward and forwards dispersion of a scalar in turbulent wall flows, International Journal of Heat and Mass Transfer, Vol. 53, 2010, pp. 1023-1035.
[12] Srinivasan, C., and Papavassiliou, D.V., Direction of scalar transport in turbulent channel flow, Physics of Fluids, Vol. 23, No. 115105, 2011, pp. 1-20.